

<sup>4</sup> Wittrick, W. H. and Williams, F. W., "A General Algorithm for Computing Natural Frequencies of Elastic Structures," *Quarterly Journal of Mechanics and Applied Maths*, Vol. 14, 1971, pp. 263-284.

<sup>5</sup> Wittrick, W. H. and Williams, F. W., "An Algorithm for Computing Critical Buckling Loads of Elastic Structures," *Journal of Structural Mechanics*, Vol. 1, 1973, pp. 497-518.

<sup>6</sup> Peters, G. and Wilkinson, J. H., "Eigenvalues of  $Ax = \lambda Bx$  with Band Symmetric  $A$  and  $B$ ," *The Computer Journal*, Vol. 12, 1969, pp. 398-404.

## Reply by Author to W. H. Wittrick

J. S. PRZEMIENIECKI\*

Air Force Institute of Technology, Wright-Patterson Air Force Base, Ohio

THE discussion of current work by Wittrick and his associates at Birmingham University is of a great interest. Not many exact solutions to complicated buckling problems are available and this work will be helpful in comparing the finite element solutions with those obtained by solving the nonlinear equations for elastic thin-walled plate structures subjected to compressive loading.

Wittrick's comment that the finite element stiffness in Ref. 1 is a special case of his exact stiffness calls for a further clarification in order to put it in proper perspective. Coefficients in the approximate stiffness matrices could, in fact, be derived by expanding the exact coefficients represented by a quotient of two complicated transcendental functions of the compressive stress  $\sigma$  and the half-wavelength  $\lambda$  and retaining only the first order terms, a monumental task in exercising one's algebraic dexterity. Only through such a manipulation can any connection between Wittrick's stiffnesses and the finite element elastic and geometric stiffnesses be established. It should also be pointed out that the two methods are based on entirely different approaches. Wittrick uses an analytical solution of the nonlinear theory of elasticity while Ref. 1 uses the standard finite element approach based on the concept of geometrical stiffness. Thus, the author's method is simply an extension of the conventional finite element technique to a special class of problems involving local instability. There is still another fundamental difference between the two methods: Wittrick's method uses the stability determinant to obtain the buckling stress which contrasts with the author's use of the standard eigenvalue equations.

The author's comment that the computational procedure for obtaining the buckling stress from the exact solution is very time consuming was simply made on the basis of the comparison of typical elements in the stiffness matrices of the two methods. For example, the stiffness coefficient for the out-of-plane plate edge rotation in the exact method, using notation of Ref. 2, is given by

$$s_{MM} = \frac{D(\xi)^{1/2}}{b} \frac{\alpha \cosh \alpha \sinh \gamma - \gamma \cosh \gamma \sinh \alpha}{\sinh \alpha \sinh \gamma + (\alpha\gamma/\omega^2)(1 - \cosh \alpha \cosh \gamma)} \quad (1)$$

for  $\xi < 1$  while for  $\xi > 1$  and  $\xi = 1$  other similar transcendental expressions are used. In these expressions  $\xi$ ,  $\alpha$ , and  $\gamma$  are functions of the stress  $\sigma$  and the half-wavelength  $\lambda$  and  $\omega$  depends on only  $\lambda$ . Equation (1) may be compared with the corresponding finite element stiffness coefficient expressed in algebraic form as

$$k_{22} = 2D \left[ \frac{\pi^4}{420} \left( \frac{b}{\lambda} \right)^3 + \frac{\pi^2}{15} \left( \frac{b}{\lambda} \right) + \left( \frac{\lambda}{b} \right) + \frac{\pi^2 \sigma t b^2}{420D} \left( \frac{b}{\lambda} \right) \right] \quad (2)$$

where the first three terms belong to the elastic stiffness matrix and the fourth term is the geometrical stiffness. Dimensionally, Eq. (2) is different from that derived by Wittrick [Eq. (1)] because

Received May 29, 1973.

Index categories: Aircraft Structural Design (Including Loads); Structural Stability Analysis.

\* Dean, School of Engineering, Associate Fellow AIAA.

his expression is for a stress-couple (in lb-in./in.) while the finite element stiffness is for a node moment (in lb-in.). Noting that an iterative solution is required to determine the half-wavelength  $\lambda$  for the lowest stress  $\sigma$  in both the exact and finite element formulations of local instability analysis, the computational simplicity of the finite element coefficients, as typically represented by Eq. (2), is quite obvious.

Reference 1 gives typical computer times for the finite element computations, but unfortunately the corresponding times for the exact method are not available to make a meaningful comparison. It should be pointed out, however, that for many problems, the finite element solutions where each component flat is treated as a single element give sufficient accuracy for engineering purposes. Furthermore, since the author's method is based on the concept of geometrical stiffness, the method may be used directly in conjunction with any finite element computer programs for the over-all instability—a definite advantage for the design engineer who needs to investigate not only the local instability but also the over-all instability of the same configuration.

The restrictive assumption that the edge lines must remain straight during buckling (the classical assumption for local instability) used in Ref. 1 can be removed and the finite element method, developed by the author, can be extended to include the in-plane stiffnesses. In fact, work is presently underway to develop the necessary matrices. This extension would permit finite element studies of coupling between long wave and short wave (local) modes of instability which can presently be accomplished with Wittrick's exact method.

Finally, regarding the comment that some of the numerical results in Fig. 5 of Ref. 1 should be above the exact curve, it should be reaffirmed that the numerical results are correct. When the biaxial stress field is compressive (both  $\sigma_x$  and  $\sigma_y$  are positive) the convergence of finite element solutions is from above; however, when the  $\sigma_y$  stress is tensile (negative  $\sigma_y$ ) and it is sufficiently high in relation to  $\sigma_x$ , the convergence is from below. The stabilizing influence of the tensile stress in the transverse direction on the strip apparently has a dominant effect on the convergence.

## References

- 1 Przemienecki, J. S., "Finite Element Structural Analysis of Local Instability," *AIAA Journal*, Vol. 11, No. 1, Jan. 1973, pp. 33-39.
- 2 Wittrick, W. H., "A Unified Approach to the Initial Buckling of Stiffened Panels in Compression," *The Aeronautical Quarterly*, Vol. 19, Pt. 3, Aug. 1968, pp. 265-283.

## Comment on "Hypersonic, Viscous Shock Layer with Chemical Nonequilibrium for Spherically Blunted Cones"

E. W. MINER\* AND CLARK H. LEWIS†  
Virginia Polytechnic Institute and State University,  
Blacksburg, Va.

IN a recent Note,<sup>1</sup> Kang and Dunn reported some of their numerical results for thin viscous shock-layer (TVSL) flows over spherically blunted cones. This Note was later supplemented

Received July 5, 1973. Work supported by NASA Contract NAS9-12630.

Index categories: Viscous Nonboundary-Layer Flows; Reactive Flows; Supersonic and Hypersonic Flows.

\* Assistant Professor, Department of Aerospace Engineering, Associate Member AIAA.

† Professor, Department of Aerospace Engineering, Associate Fellow AIAA.

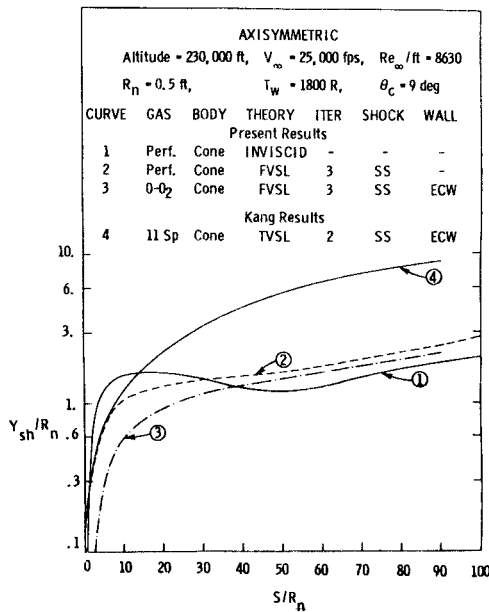


Fig. 1 Shock-layer thickness distributions for sphere-cone.

by other publications<sup>2-4</sup> giving more complete results. In their work, Kang and Dunn were principally interested in predicting electron number densities. The shock-layer governing equations were solved by an integral method and properties such as heat transfer were presented as well as electron number densities. In the reports of Kang and Dunn, one of the major points made was that the single ionizing species ( $NO^+$ ) model was inadequate to predict the ionization levels of hypersonic flows of reacting air. It appears, however, that certain flowfield results of Kang and Dunn are highly questionable.

The authors of this Comment have compared the results given by Kang and Dunn<sup>1</sup> for a 9° sphere-cone at 233,000 ft altitude and 25,000 fps with the predictions of four finite-difference methods for viscous flows and an inviscid, blunt body-method of characteristics procedure. The inviscid procedure was the combined inverse blunt body method and axisymmetric method of characteristics of Inouye, Rakich and Lomax.<sup>5</sup> The inviscid procedure predicts a shock-layer thickness ( $Y_{sh}$ ) distribution as well as the pressure distribution used by one of the two boundary-layer (BL) methods. Two of the finite-difference

methods were for boundary-layer flows; one was for perfect gas flows,<sup>6,7</sup> the other was for flows of seven specie, ( $O$ ,  $O_2$ ,  $N$ ,  $NO$ ,  $NO^+$ ,  $N_2$ , and  $e^-$ ) reacting air.<sup>8,9</sup> The other two finite-difference methods are extensions of the methods of Davis<sup>10,11</sup> for fully viscous shocklayer (FVSL) flows over nonanalytic bodies such as sphere cones; one for perfect gas,<sup>10</sup> the second for reacting, binary ( $O-O_2$ ) gas.<sup>11</sup> The finite-difference methods have been used extensively for a wide variety of conditions and have given good results.

The results of Kang and Dunn which are of particular interest to the present authors are the heat-transfer distributions and the temperature profiles. Kang and Dunn presented the temperature profiles in a nondimensional form ( $T/T_{sh}$  vs  $Y/Y_{sh}$ ). Distributions of  $Y_{sh}/R_n$  (shock-layer thickness/nose radius) and  $T_{sh}$  (temperature behind the shock) were also given and the dimensional temperature profiles could thus be obtained.

Before discussing the temperature profiles, it is appropriate to first consider the distribution of  $Y_{sh}$  and  $T_{sh}$ . Distributions of  $Y_{sh}$  are shown in Fig. 1. Results from the present shock-layer methods and from the inviscid procedure are compared with the results of Kang and Dunn. The differences in the predictions for  $S/R_n < 20$  are overshadowed by the differences in the predictions of the present methods and the method of Kang and Dunn for the downstream portion of the cone ( $S/R_n > 30$ ). While the distribution of  $Y_{sh}$  from the inviscid procedure had a different trend from the distribution predicted by the viscous shock-layer methods, the inviscid results were in substantial agreement with the present viscous results, especially for  $S/R_n > 40$ . At  $S/R_n = 90$ ,  $Y_{sh}/R_n$  was about 2 from the inviscid results and 2.5 to 3 for the present FVSL results, whereas the results of Kang and Dunn gave  $Y_{sh}/R_n = 9$ . While results obtained with the present methods for a 9° cylinder-wedge are not shown, the distribution of  $Y_{sh}$  for a wedge was quite similar to the results obtained by Kang and Dunn for a cone.

Distributions of  $T_{sh}$  are shown in Fig. 2. At the stagnation point,  $T_{sh}$  depended primarily upon the gas model used. For a perfect gas no energy is absorbed by chemical reactions and  $T_{sh}$  is higher than for a reacting gas. The value of  $T_{sh}$  for the present binary gas was very close to the value obtained by Kang and Dunn. However, on the afterbodies ( $S/R_n > 1.4$ ) the shock angle was lower than at the stagnation point and the present cone results showed the same value of  $T_{sh}$  for both the perfect gas and the binary gas. The wedge had a shock angle

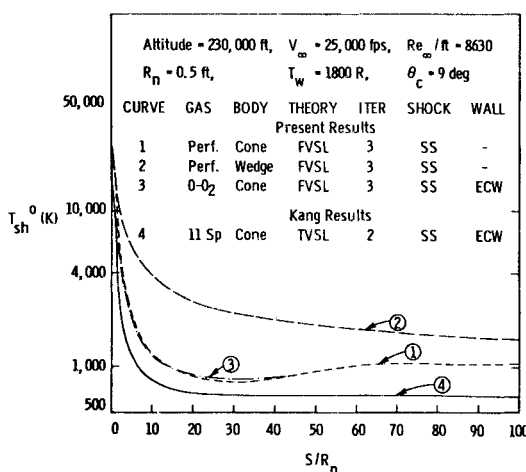


Fig. 2 Dimensional shock temperature distributions for sphere-cone and cylinder-wedge.

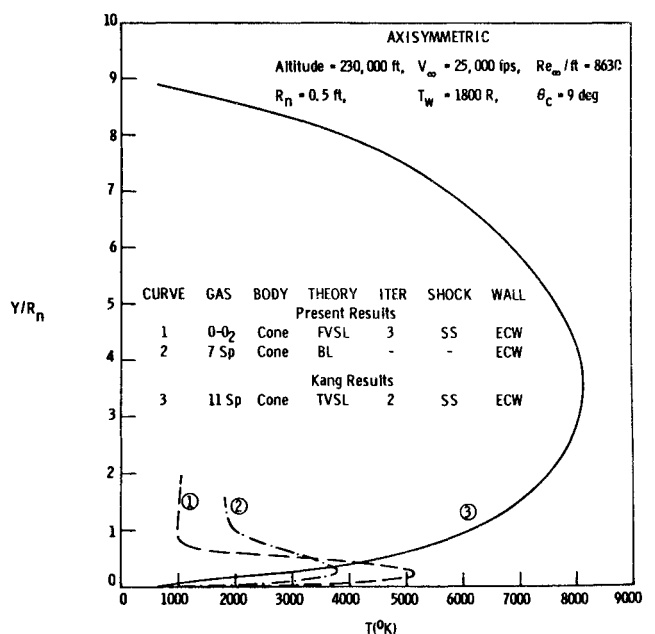


Fig. 3 Dimensional temperature profiles for sphere-cone at  $S/R_n = 90$ .

considerably greater than for the cone which gave a larger value of  $T_{sh}$ . While the present results are consistent and reasonable, comparing the present results with the results of Kang and Dunn indicates two inconsistencies in their distribution of  $T_{sh}$ . First, for their value of  $T_{sh}$  to be lower than the present cone values, the shock angle would have to be smaller. Second, for  $T_{sh}$  to be constant (at about 650°K) for  $S/R_n > 30$  this would require a constant shock angle or equivalently a constant slope for  $Y_{sh}$ . The distribution of  $Y_{sh}$  obtained by Kang and Dunn,<sup>1</sup> as shown plotted in Fig. 1, indicated that the shock-layer thickness did not have a constant slope and further indicated that the shock angle should have been greater than for the present results.

In Refs. 1, 3 and 4, Kang and Dunn claimed that their temperature profiles showed that a thin boundary layer was "recovered" far downstream. While the temperature profiles for the 9° cone case were not given in Ref. 1, they were given in Refs. 3 and 4. In Fig. 3, temperature profiles are shown for  $S/R_n = 90$ . The results of Kang and Dunn are compared with present FVSL binary gas results and with the seven specie BL results. The present viscous shock-layer results compared well with the classical boundary-layer results. Differences near the wall can be attributed to differences in chemistry; the outer-edge differences are inherent in the way edge conditions were obtained for the two methods. The present results showed that the thickness of the viscous layer was about 1 or 1.5  $R_n$  and the shock-layer method further showed an inviscid outer flow region. Comparable results were also given by the perfect gas shock-layer and boundary-layer methods. Further, while not shown, the velocity profiles predicted the edge of the viscous layer at  $Y/R_n = 1.0$  to 1.5. The results of Kang and Dunn, however, showed no inviscid outer region of the flow and also they predicted the viscous layer extended to the shock at  $Y/R_n = 9$ . The present results seem to clearly show a "recovery" of a thin boundary layer far downstream, while the results of Kang and Dunn apparently predicted a very different trend.

Distributions of heat transfer are shown in Fig. 4. The present results of the four finite-difference methods showed quite good over-all agreement for all methods, but the present results agreed poorly with the results of Kang. At the stagnation point the results of Kang were lower than the present results (although the amount is not fully shown) while downstream ( $S/R_n > 20$ ) the method of Kang and Dunn predicted a heat transfer three times that given by the present methods. The values of heat transfer at the stagnation point are given in Table 1. In Table 1 the following nomenclature is used, ECW is equilibrium catalytic wall, SS is shock slip. Some differences in stagnation heat transfer would be expected on the basis of differences in flowfield models and gas chemistry. The differences between the present results and the results of Kang and Dunn, especially the differences in the trends of the results, are not readily explained by differences in flowfield models or gas chemistry.

**Table 1 Stagnation heat-transfer for sphere-cone, 230,000 ft conditions**

Model	Gas	Wall	Shock	$\dot{q}$ , BTU/ft <sup>2</sup> -sec
Present results				
BL	PG	...	...	231.074
BL	7 sp	ECW	...	177.25
FVSL	PG	...	SS	123.973
FVSL	O-O <sub>2</sub>	ECW	SS	238.742
TVSL	7 sp	ECW	SS	252.539
Kang results				
TVSL	11 sp	ECW	SS	87.772

The results discussed in this Comment, showed consistently large differences between the present results and the results of Kang and Dunn. As, or more, important were the differences

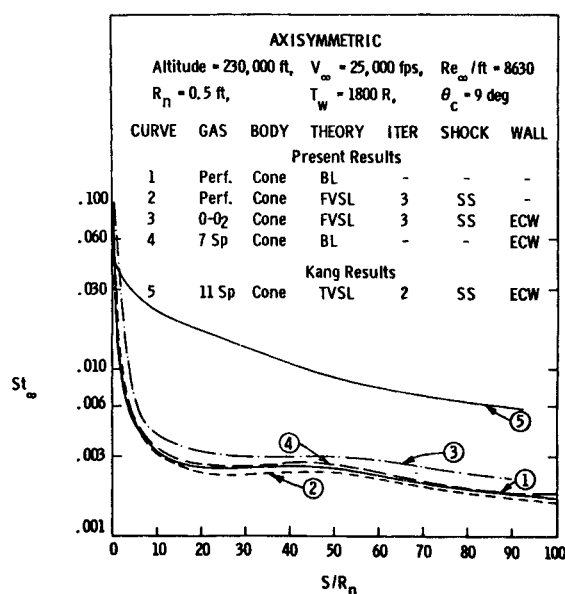


**Fig. 4 Heat-transfer distributions for sphere-cone.**

in the trends of the results. Because the methods used for the present analysis were largely independent and previous results from the present methods have consistently compared well with both experimental data and other numerical results, we believe the good agreement among the several present methods should give our results considerable credibility. The present results strongly indicate that differences as large as those between the present results and the results of Kang and Dunn could not be due to differences in gas chemistry. If the results of Kang and Dunn were as much in error as the present results indicate, of necessity the electron number density concentrations which they obtained would have been affected because of the dependency on the temperature profiles.

## References

- Kang, S.-W. and Dunn, M. G., "Hypersonic, Viscous Shock Layer with Chemical Nonequilibrium for Spherically Blunted Cones," *AIAA Journal*, Vol. 10, No. 10, Oct. 1972, pp. 1361-1362.
- Kang, S.-W., Jones, W. L., and Dunn, M. G., "Theoretical and Measured Electron-Density Distributions at High Altitudes," *AIAA Journal*, Vol. 11, No. 2, Feb. 1973, pp. 141-149.
- Kang, S.-W. and Dunn, M. G., "Hypersonic, Viscous Shock Layer with Chemical Nonequilibrium for Spherically Blunted Cones," TR AF-3093-A-1, Feb. 1972, Cornell Aeronautical Lab., Buffalo, N.Y.
- Dunn, M. G. and Kang, S.-W., "Theoretical and Experimental Studies of Reentry Plasmas," CR-2232, April 1973, NASA.
- Inouye, M., Rakich, J., and Lomax, H., "A Description of Numerical Methods and Computer Programs for Two-Dimensional and Axisymmetric Supersonic Flow over Blunt Nosed and Flared Bodies," TN D-2970, Aug. 1965, NASA.
- Anderson, E. C. and Lewis, C. H., "Laminar or Turbulent Boundary-Layer Flows of Perfect Gases or Reacting Gas Mixtures in Chemical Equilibrium," CR-1893, 1971, NASA.
- Lewis, C. H., Anderson, E. C., and Miner, E. W., "Nonreacting and Equilibrium Chemically Reacting Turbulent Boundary-Layer Flows," AIAA Paper 71-597, Palo Alto, Calif., 1971.
- Lewis, C. H., Adams, J. C., and Gilley, G. E., "Effects of Mass Transfer and Chemical Nonequilibrium on Slender Blunted Cone Pressure and Heat Transfer Distributions at  $M_\infty = 13.2$ ," TR-68-214, Dec. 1968, Arnold Engineering Development Center, Tullahoma, Tenn.
- Lewis, C. H. and Miner, E. W., "Stagnation Point Viscous Layers with Mass Transfer," *Computers and Fluids*, to be published, 1973.
- Davis, R. T., "Numerical Solution of the Hypersonic Viscous Shock-Layer Equations," *AIAA Journal*, Vol. 8, No. 5, May 1970, pp. 843-851.
- Davis, R. T., "Hypersonic Flow of a Chemically Reacting Binary Mixture Past a Blunt Body," AIAA Paper 70-805, Los Angeles, Calif., 1970.